Molecular Vision 2005; 11:1151-65 <http://www.molvis.org/molvis/v11/a133/>
Received 16 June 2005 | Accepted 17 December 2005 | Published 21 December 2005

RPE65 surface epitopes, protein interactions, and expression in rod- and cone-dominant species

Nahid Hemati,[1] Kecia L. Feathers,[1] Jared D. Chrispell,[1,2] David M. Reed,[1] Thomas J. Carlson[1] Debra A. Thompson[1,2]

(The first two authors contributed equally to this publication)

Departments of [1]Ophthalmology and Visual Sciences and [2]Biological Chemistry, University of Michigan Medical School, Ann Arbor, MI

Purpose: RPE65 is an abundant protein necessary for the synthesis of the chromophore 11-*cis* retinal by the retinal pigment epithelium (RPE). Our purpose was to identify RPE65 surface epitopes, to assess protein interactions, and to evaluate RPE65 expression in eyes from rod- and cone-dominant species using a monoclonal antibody approach.
Methods: RPE65-specific monoclonal antibodies, mAb 8B11, and mAb 1F9, were generated using bovine RPE microsomal membranes and a human RPE65 synthetic peptide as immunogen, respectively. Western analysis was performed on bovine RPE membranes, as well as yeast strains generated by transfection with *RPE65* cDNAs. Competition of antibody binding by synthetic peptides was assayed using ELISAs, western analysis, and elution from immunoaffinity matrices. RPE65 structural models were generated by ab initio and comparative methods. Immunohistochemistry was performed on retina/RPE/choroid cryosections and retina flatmounts.
Results: The antigenic determinant recognized by mAb 8B11 was localized to a 10 amino acid sequence, KVNPETLETI, that competed binding with μM affinity and eluted RPE65 from an immunoaffinity matrix incubated with solubilized bovine RPE membranes or RPE65-transfected cells. Similarly, solubilized RPE65 was bound and eluted from an mAb 1F9 immunoaffinity matrix using the immunizing peptide, FHHINTYEDNGFLIV. In both cases, 11-*cis* retinol dehydrogenase, but not other known visual cycle proteins, appeared to co-elute with RPE65 in substoichiometric amounts. Both sequences localized to surface exposed regions of predicted RPE65 tertiary structures. RPE65 immunoreactivity was detected by mAb 8B11 and mAb 1F9 in the RPE, but not in retina, in bovine, rat, mouse, human, chicken, and *Xenopus laevis*, and in *Nrl* knockout mice whose retinas contain exclusively cone-like photoreceptor cells.
Conclusions: The identification of RPE65 surface exposed antigenic determinants represents a first step toward understanding RPE65 structure and its interaction with visual cycle proteins, and provides a means for the purification of the native protein. The finding that RPE65 immunoreactivity is present in the RPE and not retina of both rod- and cone-dominant species does not support a proposed direct role for RPE65 in cone cell function.

RPE65 is an abundant protein expressed in the RPE where it functions in the visual cycle necessary for the synthesis of 11-*cis* retinal, the chromophore of the visual pigments [1,2]. Developmentally, RPE65 is an important marker for the differentiated phenotype of the RPE [3]. Mutations in the gene encoding *RPE65* are responsible for childhood-onset forms of autosomal recessive severe retinal dystrophy, including Leber congenital amaurosis, in an estimated 11% of cases [4]. A number of research groups are currently involved in efforts to develop therapeutic methods specific for RPE65 loss-of-function [5-7], with clinical trials of gene replacement therapy planned for the near future.

Correspondence to: Debra A. Thompson, PhD, University of Michigan Medical School, W. K. Kellogg Eye Center, 1000 Wall Street, Ann Arbor, MI, 48105; Phone: (734) 936-9504; FAX: (734) 647-0228; email: dathom@umich.edu

T. J. Carlson is now at the Department of Biochemistry, Pfizer Global Research and Development, La Jolla Laboratories, San Diego, CA

Recent studies show that RPE65 functions as the isomerohydrolase in the RPE that converts all-*trans* retinyl esters to 11-*cis* retinol [8-10] by coupling the free energy of ester hydrolysis to the *trans* to *cis* isomerization reaction [11]. This role is compatible with the findings of earlier studies showing that RPE65 is a retinoid-binding protein [12,13] that acts a molecular switch, binding all-*trans* retinyl esters when palmitoylated, and all-*trans* retinol when depalmitoylated by transfer to lecithin retinol acyl transferase (LRAT) [14]. Pathogenesis associated with RPE65 loss-of-function is proposed to result, in part, from constitutive opsin activity due to loss of chromophore [15], although other interpretations exist [16]. More than half of all known *RPE65* mutations are missense substitutions affecting over 30 different amino acid residues [4].

The relatively high incidence of *RPE65* mutations in patients with early-onset disease, as well as its central role in current therapeutic efforts, creates a strong incentive to achieve a mechanistic understanding of RPE65 participation in the visual cycle. Among the many critical issues to resolve include elucidating the mechanism(s) by which missense mutations

disrupt RPE65 function, and establishing the role of RPE65 in rod- and cone-associated visual cycles. Cones have been proposed to have a private pathway of regeneration that may involve their ability to oxidize 11-*cis* retinol to 11-*cis* retinal [17,18]. RPE65 has been proposed to directly participate in the cone visual cycle based on its reported expression in cones [19].

For studies of RPE65 expression, function, and structure, we developed monoclonal antibodies specific for RPE65. One of these, mAb 8B11, elicited using RPE membranes as immunogen, has been widely distributed and used in various applications [20-24]. A second antibody, mAb 1F9, was elicited using an RPE65 synthetic peptide. We now report the identification of the mAb 8B11 antigenic determinant, demonstrate its usefulness for RPE65 immunoaffinity purification, and characterize the pattern of RPE65 immunoreactivity in eyes from rod- and cone-dominated species.

METHODS

Synthesis of RPE65 synthetic peptides: The antigenic index for RPE65 was calculated using the Jameson-Wolf prediction of the Protean module in Lasergene suite of software (DNA STAR, Inc., Madison, WI). Peptides of interest were synthesized by the University of Michigan Protein Facility. For use as immunogen, peptide 312-FHHINTYEDNGFLIV-326 (corresponding to human RPE65), was synthesized with an added carboxy-terminal cysteine residue and conjugated to keyhole limpet cyanin (KLH) using Imject Maleimide Activated Immunogen Conjugation Kit (Pierce Chemical Co., Rockford, IL) according to manufacturer's instructions. Peptides were similarly conjugated to ovalbumin for use as substrates in ELISAs. For use in competition assays of mAb 8B11 binding, synthetic peptides corresponding to five regions having the highest predicted antigenicity within bovine RPE65 sequence from Phe108 to Lys236 (RPE65 Region 2; see below) were synthesized: Peptide 1 (Phe108 to Phe116), Peptide 2 (Val126 to Leu133), Peptide 3 (Ile152 to Asp167), Peptide 4 (His182 to Asn191), Peptide 5 (Gln213 to Glu224); and also Peptides 6-9 that were derived from Peptide 3 by deletion of N- and C-terminal residues. For assessing nonspecific effects, RPE65 peptide 93-MTEKRIVITE-102 (peptide 18), was synthesized.

mAb production and screening: The protocol used for mAb production adhered to the ARVO Statement for the Use of Animals in Ophthalmic and Vision Research. Six-week-old Balb/c female mice were immunized by intraperitoneal injection with 40 μg of KLH-conjugated peptide FHHINTYEDNGFLIV, or with 40 μg of a membrane fraction enriched in RPE microsomal membranes obtained by sorbitol gradient centrifugation [25] from bovine RPE cells isolated by Ficoll gradient centrifugation [26]. A minimum of three immunizations in adjuvant were given at three week intervals, and fusions were performed using standard procedures [27,28] and the AGA-X63.653 cell line [29]. Hybridoma supernates were screened by ELISA using bovine RPE membranes or peptide FHHINTYEDNGFLIV conjugated to ovalbumin as substrates, and subsequently screened by western and immunohistochemical analysis, as described below. For western analysis, bovine RPE and mouse RPE/choroid membrane proteins were separated by SDS-PAGE, transferred to nitrocellulose, and incubated with primary and secondary antibody (alkaline phosphatase-conjugated) using standard methods [30]. Typing of antibody class and subclass was performed using ImmunoPure Monoclonal Antibody Isotyping Kit (Pierce Chemical Co., Rockford, IL) according to manufacturer's instructions. Hybridomas producing RPE65 antibodies were expanded and grown in culture for six weeks prior to harvest. IgG was isolated from ascites fluid obtained from in vivo hybridoma cultures using chromatography on DEAE-Sepharose in high salt [31] or protein-A Sepharose (Prosep A kit, Millipore Corp., Billerica, MA).

Immunohistochemical analysis: For cryosections, eyes were fixed in cold 4% paraformaldehyde (mice and rats were first perfused with PBS, then 4% paraformaldehyde), washed in PBS, transitioned to sucrose/OCT, frozen in dry-ice cooled hexanes, and 10 μm sections cut through the retina/choroid/RPE (for large eyes) or whole globes (for small eyes). For mAb 8B11, sections (except mouse) were blocked with 20% sheep serum and 0.2% Triton X-100 (Sigma-Aldrich, St. Louis, MO) in PBS, incubated with mAb 8B11 (2 μg/ml) for 2 h, then with Alexa Fluor 555-conjugated anti-mouse IgG (1:500, Molecular Probes, Inc., Eugene, OR) for 1 h. For mouse sections with mAb 8B11, and all sections with mAb 1F9 (30 μg/ml), the Mouse on Mouse (M.O.M.) Peroxidase kit (Vector Laboratories, Burlington, CA) was used for blocking and antibody incubation (1 h at RT), and the TSA-Alexa fluor 568 kit (Molecular Probes, Inc.) was used for visualization.

For retina flatmounts, mouse eyes were enucleated and the retinas dissected and fixed in cold 4% paraformaldehyde for 1 h. Immunohistochemistry and lectin labeling was performed essentially as in [19]. In brief, retinas were washed in PBS, blocked with 20% sheep serum, 0.2% Triton X-100 in PBS, incubated with mAb 8B11 or mAb 1F9 and FITC-conjugated PNA-lectin (0.05 mg/ml, Molecular Probes, Inc.) in 2% sheep serum, 0.2% Triton X-100 in PBS for 12 h, washed and incubated in the same buffer with Alexa Fluor 555-conjugated anti-mouse IgG (1:500) for 12 h. Alternatively, retinas were incubated with mAb 8B11 (2 μg/ml) and rabbit anti-S-opsin (1:500) or anti-M/L-opsin (1:500, Chemicon International, Inc., Temecula, CA) for 12 h, then with Alexa Fluor 555-conjugated anti-mouse IgG (1:500) and Alexa Fluor 488-conjugated anti-rabbit IgG (1:400) for 12 h.

Specimens were viewed and photographed on a Nikon Eclipse E800 microscope with a Nikon DMX1200 digital camera using the manufacturer's data acquisition software. Phase contrast and fluorescence images were obtained (FITC-PNA lectin, 488 nm; Alexa Fluor, 555 and 568 nm). The approximate ages of the eyes used for immunohistochemical analysis were: human, 49 year; bovine, 4 months; wild type (B6/129) mouse, 40 days; Rpe65 knockout mouse, 50 days; Nrl knockout mouse, 42 days; rat, 6 months; *Xenopus laevis*, 4 week; and chicken, 4 months.

Expression and mAb 8B11 analysis of RPE65 *fusion constructs:* Total RNA from bovine RPE cells was isolated using CsCl centrifugation [32] and *RPE65* cDNA sequences were

amplified as five fragments of about 300 bp (Region 1, Met1-Ala107; Region 2, Phe108 to Lys236; Region 3, Lys236-Phe312; Region 4, His314-Pro419; Region 5, Gln420-Ser533) using reverse transcriptase coupled polymerase chain reaction (primer sequences available on request). The cDNAs were cloned into pHybLex/Zeo (Invitrogen, Carlsbad, CA) to generate expression constructs, and yeast strains expressing the fusion proteins were made by transfection of L40 cells using electroporation. The cells were grown at 30 °C overnight, lysed in 8 M urea and 5% SDS, 40 mM Tris HCl, pH 6.8, 0.1 mM EDTA, and 1% β-mercaptoethanol. Soluble proteins were separated by SDS-PAGE, transferred to nitrocellulose, and probed with anti-LexA antibody (Invitrogen) or with mAb 8B11 IgG.

Competition assays of mAb 8B11 binding with synthetic peptides: Peptide competition of mAb 8B11 binding was evaluated using ELISAs [33]. In brief, bovine RPE membranes [34] were dried down in microtitre plates (6 μg protein/well), and blocked with 5% BSA, 0.05% Tween-20, and 0.02% sodium azide in PBS. Synthetic peptides at range of concentrations (0.1 to 100 μM) were incubated with mAb 8B11 (0.3 μg IgG/ml) in 0.1% BSA, 0.05% Tween-20 in PBS at RT for 1 h, then incubated in the microtitre plates overnight. The plates were washed, incubated with horseradish peroxidase-conjugated mouse IgG (1:2500; Sigma-Aldrich), washed and developed using 5-amino salicylic acid (Sigma-Aldrich). Absorbance was measured at 550 nm using a Spectra Max 190 plate reader (Molecular Devices Corp., Sunnyvale, CA).

For western analysis of peptide competition of mAb 8B11 binding, nitrocellulose blots of bovine RPE membrane proteins separated by SDS-PAGE were incubated with mAb 8B11 (0.3 μg IgG/ml) that was preincubated with 100 μM peptide in primary antibody solution [30] for 2 h at RT, and the blots were then processed as described above.

Immunoadsorption and peptide elution: Affinity matrices were generated by crosslinking mAb 8B11 or mAb 1F9 to CNBr-activated Sepharose 4B (Amersham Biosciences, Piscataway, NJ) according to manufacturer's instructions. Bovine RPE membranes (200 μg) were solubilized in 10 mM sodium phosphate, 150 mM NaCl, pH 7.0, and Complete protease inhibitors (Roche Diagnostics Corp., Indianapolis, IN) containing either 0.8% CHAPS, 0.8% octylglucoside, 0.5% laurylmaltoside, or 0.5% Genapol. The solubilized membranes were incubated with affinity matrix (50 μl) overnight at 4 °C, then washed and eluted by incubation with 500 μM peptide (100 μl) for 1 h at RT in the same detergent solution used for solubilization, but at lower concentrations (0.7% CHAPS, 0.7% octylglucoside, 0.2% laurylmaltoside, or 0.2% Genapol). The eluted proteins were analyzed by SDS-PAGE, coomassie blue staining, and western analysis using mAb 8B11 or mAb 1F9, and antibodies against 11-*cis* retinal dehydrogenase (RDH5) [35], the retinal G protein-coupled receptor (RGR) [36], and lecithin retinol acyl transferase (tLRAT) [37].

For studies of the recombinant protein, COS-7 cells were transiently transfected with human *RPE65* cDNA in a derivative of the mammalian expression vector pMT2 [38], or with empty vector, using FuGENE6 (1 μg DNA/3 μl reagent in 6 well plates) according to the manufacturer's instructions (Roche Diagnostics Corp.). Cells were harvested at 44 h post-transfection and immunoadsorption experiments were performed using the conditions described for bovine RPE membranes.

Generation of predicted RPE65 tertiary structures: A low-resolution model of the tertiary structure of the RPE65 protein was derived, ab initio, by submitting the human RPE65 amino acid sequence (GenBank AAA99012) to the automated I-sites/HMMSTR/Rosetta server [39]. The server automates a process of modeling tertiary structure from amino acid sequence using HMMSTR, a hidden Markov model based on protein structures in the invariant or initiation folding sites (I-sites) library of nonredundant short sequence motifs (supersecondary structures) that correlate with local structures [40], coupled with the Rosetta program to build structures from protein fragments [41]. The resulting tertiary structure with predicted coordinates was visualized and displayed with Discover Studio ViewerPro 5.0 (Accelrys, San Diego, CA).

A second model of RPE65 tertiary structure was generated using the recently solved structure of the apocarotenoid-

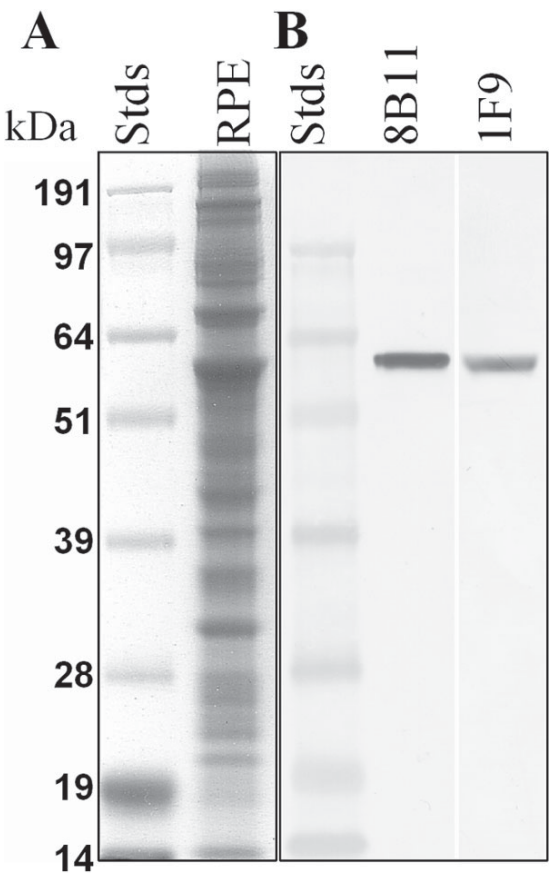

Figure 1. Immunoreactivity of mAb 8B11 and mAb 1F9 with bovine RPE membranes. **A**: Coomassie blue staining of proteins separated by SDS-PAGE (20 μg protein). **B**: Western analysis (1 μg protein) of proteins separated by SDS-PAGE, transferred to nitrocellulose, incubated with mAb 811 (0.2 μg/ml), or mAb 1F9 (3 μg/ml), and immunoreactivity visualized using alkaline phosphatase coupled anti-mouse IgG. RPE65 migrates at about 61 kDa.

cleaving oxygenase from *Synechocystis* sp. PCC 6803 (PDB 2biw:a) as a template; a member of the retinal-forming carotenoid oxygenases protein family of which RPE65 and β-carotene-15, 15'-oxygenase are members [42]. Using the functions for matching and aligning available in Swiss-PDBViewer/DeepView (version 3.71b1), the human RPE65 amino acid sequence was placed into the structure of PDB 2biw and the resulting file was submitted to the SWISS-MODEL server [43]. The resulting tertiary structure with coordinates was displayed and annotated with DS ViewerPro.

RESULTS

Antibody development: In screens of hybridomas generated from mice immunized with bovine RPE membranes, clone 8B11 (IgG1 kappa) was found to produce a high-affinity monoclonal antibody specific for RPE65 in western analysis of bovine RPE membranes (Figure 1). Specificity for RPE65 was further demonstrated by comparison of immunoreactivity in

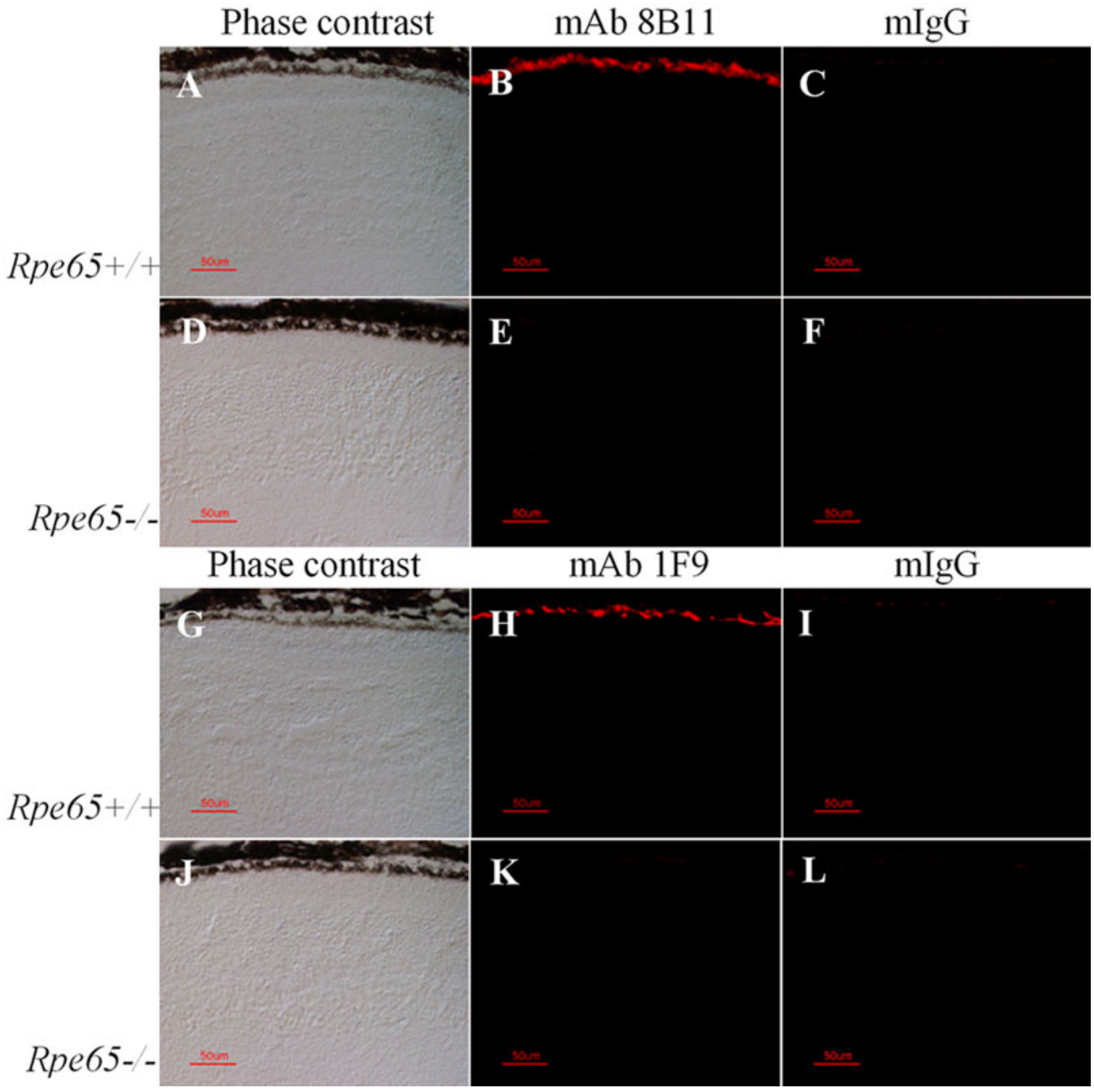

Figure 2. Immunohistochemical analysis of mAb 8B11 and mAb 1F9 reactivity in wild type and *Rpe65* knockout mice. Cryosections were incubated with mAb 8B11 (2 μg/ml) or mAb 1F9 (30 μg/ml) using M.O.M. Peroxidase reagents, with visualization using TSA-Alexa fluor 568 reagents and using fluorescence imaging (1/30 s). Phase contrast images (**A**,**D**,**G**,**J**); mAb reactivity (**B**,**E**,**H**,**K**); non-immune mIgG reactivity (**C**,**F**,**I**,**L**).

mouse eye sections from wild type and *Rpe65* knockout mice that showed reactivity only in the RPE of the wild type animals (Figure 2, top). Similarly, immunization of mice with the human RPE65 peptide, 312-FHHINTYEDNGFLIV-326, resulted in the identification of a hybridoma producing a monoclonal antibody, 1F9 (IgG1 kappa), specific for RPE65 in westerns of bovine RPE membranes (Figure 1) and in immunohistochemical analysis of wild type *Rpe65* knockout mice (Figure 2, bottom). However, the working concentrations of mAb 1F9 needed were at least 10 fold greater than those for mAb 8B11, indicative of the relatively lower affinity of mAb 1F9 for the bovine and mouse proteins.

mAb 8B11 epitope mapping: To identify the region of RPE65 sequence recognized by mAb 8B11, bovine *RPE65* cDNA was cloned into pHybLex/Zeo as five partial sequences (Regions 1-5, Figure 3) and expressed as LexA-fusion proteins in yeast. Each of the five fusion proteins, as well as the full-length sequence, was positive when probed with anti-LexA antibody in western analysis (Figure 4A). However, only Region 2, encompassing RPE65 residues F108 to K236, and the full-length fusion protein were positive for mAb 8B11 reactivity (Figure 4B).

To localize the antigenic determinant within Region 2, competition ELISAs using synthetic peptides were performed. Peptides 1-5 corresponding to RPE65 sequences having the highest antigenic indices and surface probabilities within Region 2 (Figure 3) were synthesized and evaluated at a range of concentrations for their ability to compete mAb 8B11 binding

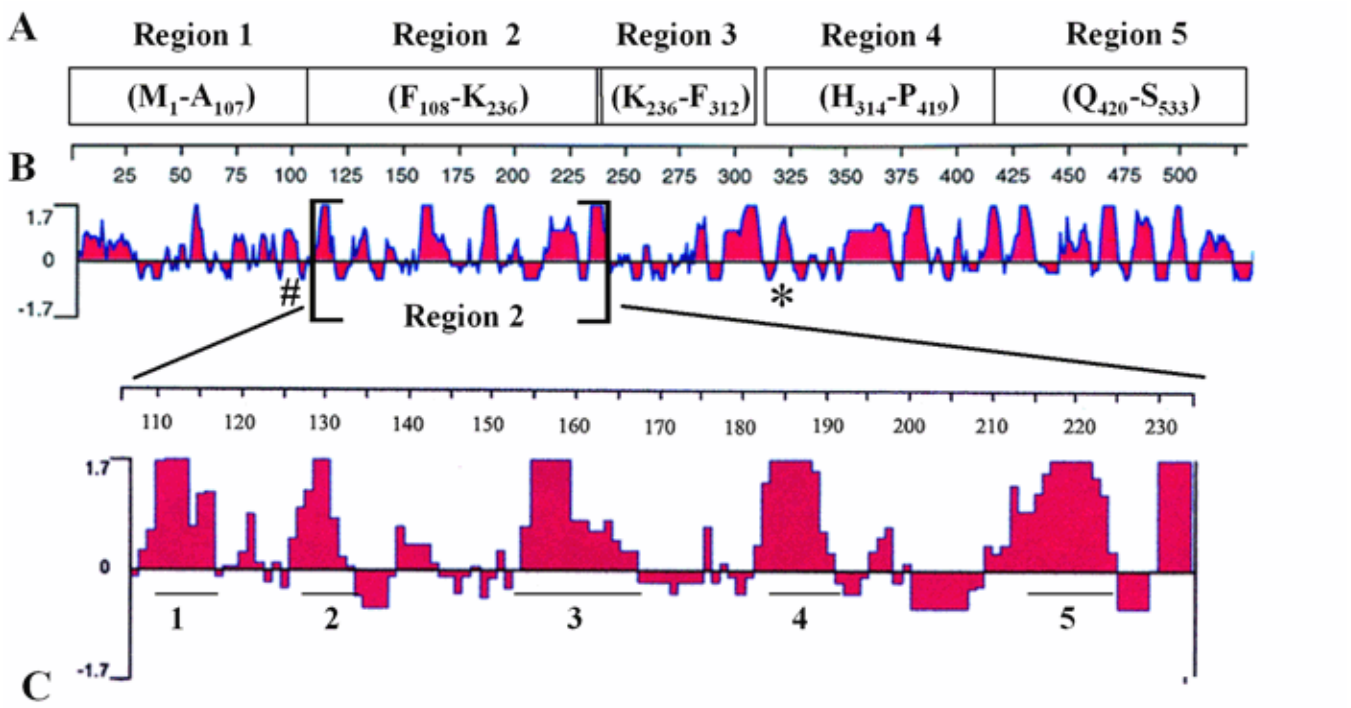

Figure 3. Schematic of RPE65 amino acid sequence. **A**: Protein fragments (Regions 1-5) encoded by RPE65 partial cDNAs cloned into pHybLex/Zeo constructs used for expression of fusion proteins in yeast. **B**: RPE65 antigenic index calculated using the Jameson-Wolf prediction in the DNASTAR program Protean. Positions of synthetic peptides 1-5 corresponding to the five sequences of highest predicted antigenicity in Region 2 (F108 to K236) are shown underlined in the enlarged section. **C**: Amino acid sequences of the synthetic peptides used in this study.

to native RPE membranes in ELISAs. Peptide 3, consisting of RPE65 residues I152 to D167, competed mAb 8B11 binding with high affinity (IC_{50} about 0.4 μM, Figure 5A). No significant competition by any of the other four peptides was observed. In a second set of ELISAs performed using peptides derived from peptide 3 by deleting residues from the amino and carboxyl terminal ends, loss of the first 4 amino acids (peptide 7; N156-D167) or the final 6 amino acids (peptide 8; I152-E161) was found to greatly reduce the ability to compete mAb 8B11 binding (Figure 5B). However, deletion of the final 4 residues (peptide 6; I152-I163) and the first 2 residues (peptide 9; K154-I163) did not decrease the ability to compete, with approximately equal concentrations of peptide 3, and internal peptides 6 and 9, required for half maximal inhibition (IC_{50} about 0.4-0.5 μM).

Peptides from RPE65 Region 2 were also tested for their ability to compete mAb 8B11 binding to denatured proteins using western analysis. Only peptide 3, and internal peptides 6 and 9, decreased mAb 8B11 binding to RPE65 when included in incubations of blots of bovine RPE proteins (Figure 5C). Taken together, the results ELISA and western analysis suggest that the epitope recognized by mAb 8B11 corresponds to a linear amino acid sequence including all or most peptide KVNPETLETI.

RPE65 affinity purification: To determine whether the epitopes recognized by mAb 8B11 and mAb 1F9 are accessible on the surface of RPE65, and to establish a mechanism for purifying the native protein, bovine RPE membranes solubilized in non-ionic detergents were incubated with immunoaffinity matrices, followed by elution with various RPE65 peptides.

When RPE membrane proteins were incubated with a mAb 8B11 affinity matrix, RPE65 could be bound and specifically eluted by incubation with peptides containing the KVNPETLETI sequence, appearing as a 61 kDa band on coomassie blue stained gels. Results obtained using CHAPS and elution with peptide 9 are shown in Figure 6A. Peptide 18, an unrelated peptide from Region 1, was used a control for nonspecific elution. Comparable results were obtained using laurylmaltoside, octylglucoside, or Genapol, with the identity of RPE65 confirmed by western analysis (Figure 6D). The amount of RPE65 recovered by peptide elution was somewhat less than when the affinity matrix was eluted by stripping with SDS sample buffer. However, elution with SDS sample buffer also resulted in the release of small amounts of IgG light chain (MW about 25 kDa) from the matrix (presumably due to reduction of intramolecular disulfide linkages), as well as trace amounts of nonspecifically bound protein. Residual RPE65 remaining on the matrix following elution with KVNPETLETI-containing peptides was also released by SDS stripping, suggesting that RPE65 undergoes significant hydrophobic interaction with the solid support, a situation also

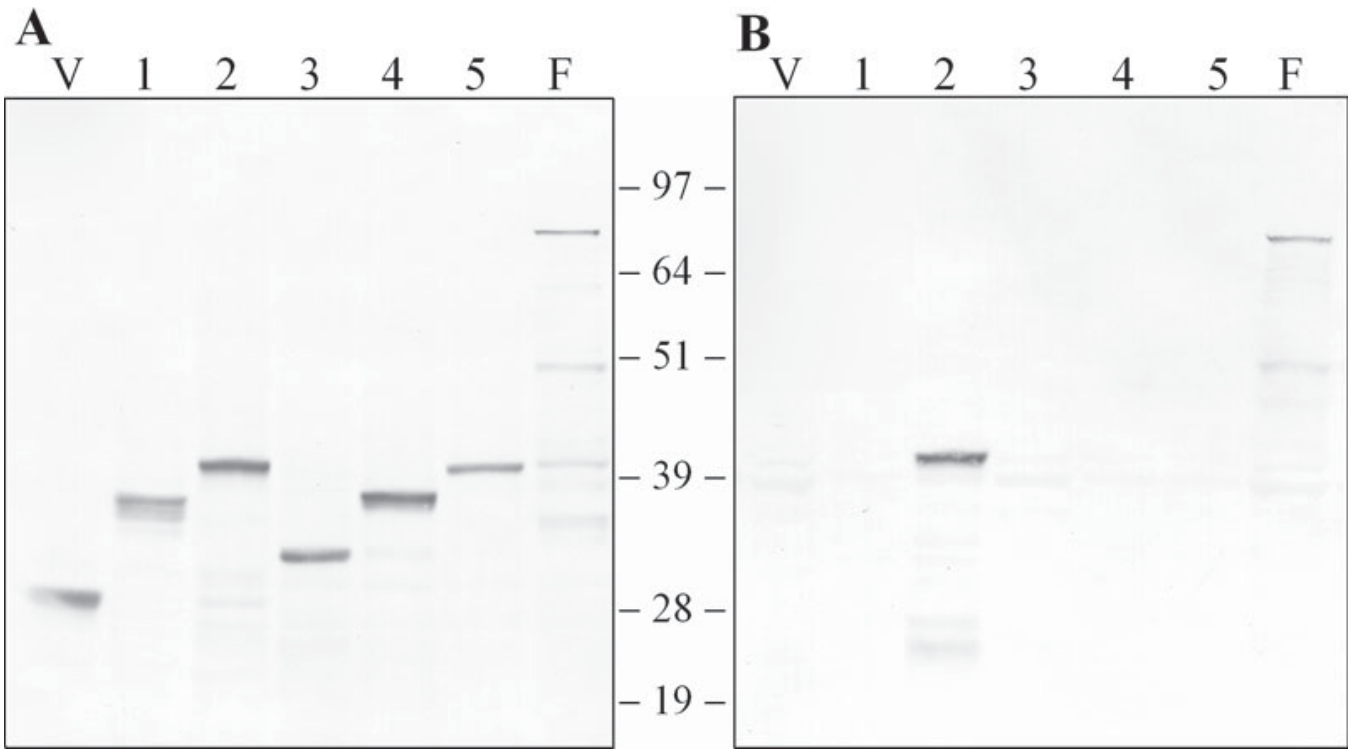

Figure 4. Immunoreactivity of RPE65-fusion proteins. Western analysis of yeast strains transfected with RPE65-pHybLex/Zeo expression constructs encoding RPE65 Regions 1-5 shown in Figure 3. Soluble proteins from cells lysed in 8 M urea and 5% SDS were separated by SDS-PAGE and transferred to nitrocellulose. Blots were probed with anti-LexA antibody (**A**) or mAb 8B11 (**B**), and reactivity visualized using alkaline phosphatase coupled anti-mouse IgG. The vector is in the lane labeled "V", the full length RPE65 cDNA is in the lane labeled "F", and regions 1-5 are in the numbered lanes.

observed using a non-immune mouse IgG affinity matrix. The mAb 8B11 affinity matrix was also effective for purifying recombinant RPE65 from COS-7 cells transfected with human *RPE65* cDNA, using conditions similar to those for bovine RPE. Purified rRPE65 appeared as a single band on coomassie blue stained gels (Figure 6B).

Similar results were obtained for purification of RPE65 from bovine RPE membranes using the mAb 1F9 affinity matrix eluted with the FHHINTYEDNGFLIV peptide, with some differences (Figure 6C,E). The mAb matrix was effective at binding RPE65, however incubation with nonspecific peptides resulted in leaching of RPE65 from the matrix, and total yields of purified protein were significantly less than obtained with mAb 8B11; both effects presumably due to the lower apparent affinity of mAb 1F9 for bovine RPE65. In addition, purification trials using the non-ionic detergent Genapol were not successful.

The finding that affinity matrices made using either mAb 8B11 or mAb 1F9 are effective for immunoadsorption of RPE65 solubilized in non-ionic detergent is consistent with the interpretation that the corresponding antigenic amino acid sequences are located on the surface of the native protein.

Visual cycle proteins co-purified with RPE65: Although RPE65 preparations obtained by affinity purification appeared to be relatively pure on coomassie blue-stained gels, western analysis was used to assess whether visual cycle proteins that potentially associate with RPE65 in vivo were co-eluted in our protocols. Blots of the proteins eluted from the mAb 8B11 matrix with peptide 9 and probed with an antibody against 11-*cis* retinal dehydrogenase (RDH5; about 35 kDa) [35] showed that small amounts of RDH5 co-eluted with RPE65 in all four detergents tested (Figure 6D, bottom). Trace amounts of RDH5 were also seen on blots of the proteins eluted from the mAb 1F9 matrix using FHHINTYEDNGFLIV in laurylmaltoside (Figure 6E, bottom). For both mAb 8B11 and mAb 1F9 matrices, as well as non-immune IgG matrix, RDH5 in significant amounts was seen in SDS-sample buffer eluates, consistent with nonspecific interactions of RDH5 with the solid support. In contrast, western analysis using antibodies against RGR [36] and LRAT [37] did not detect the corresponding proteins in peptide eluates of either mAb 8B11 or mAb 1F9 matrix (data not shown).

Predicted tertiary structure and epitope placement: Two approaches were used to generate structural models of RPE65 useful for experimental interpretation and design. First, a low-resolution tertiary structure for RPE65 was predicted from the primary sequence using the I-sites/HMMSTR/Rosetta server [39] that automates the use of protein folding rules to predict local, secondary, and supersecondary structures using a Markov state to represent a position in an I-site motif [40], coupled with the Rosetta program to build structures from protein fragments using a Monte Carlo simulated annealing algorithm [41] (Figure 7). A second model was generated based on the recently solved structure of the apocarotenoid-cleaving oxygenase from *Synechocystis* sp. PCC 6803 [PDB 2biw:a], a member of the retinal-forming carotenoid oxygenase family that contains RPE65 and β-carotene-15, 15'-oxygenase [42]. In DeepView, the RPE65 sequence was aligned and fit to the PDB 2biw sequence, the resulting structure was further modeled by the SWISS-MODEL server, and the coordinates annotated in DS ViewerPro [43] (Figure 8). The resulting RPE65 structures with predicted coordinates were displayed and annotated to highlight the epitope recognized by mAb 8B11 and mAb 1F9, and the locations of the amino acid substitutions resulting from patient missense mutations.

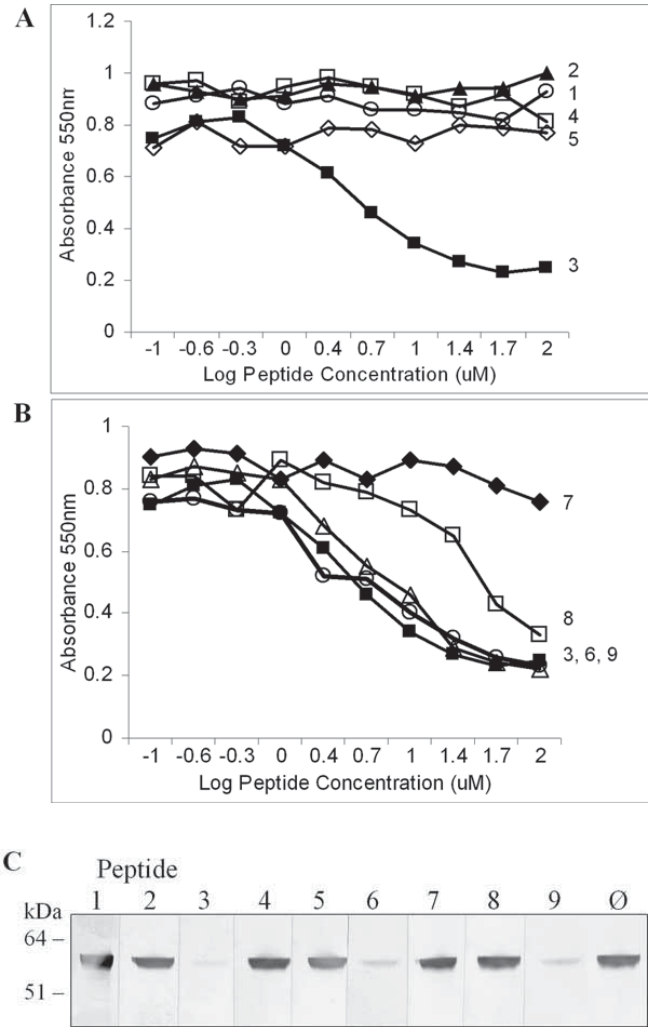

Figure 5. Peptide competition of mAb 8B11 binding. **A**,**B**: Competition ELISA of mAb 8B11 binding with synthetic peptides corresponding to sequences in RPE65 Region 2. RPE membranes in microtitre plates were incubated with mAb 8B11 plus peptides at concentration range of 0.1 to 100 μM. **A**: Competition with peptide 1 are circles, 2 are triangles, 3 are black rectangles, 4 are white rectangles, 5 are rhomboids (sequences shown in Figure 3). **B**: Competition with derivatives of peptide 3 (black rectangles) made by deleting residues from the amino (peptide 7, rhomboids) or carboxyl (peptide 6, triangles; peptide 8, white rectangles) ends, or both (peptide 9, white rectangles). Data are representative of three independent experiments. **C**: Western analysis of peptide competition of mAb 8B11 binding. Bovine RPE membrane proteins separated by SDS-PAGE and blotted on nitrocellulose were incubated with mAb 8B11 plus various peptides (100 μM) as shown, and reactivity visualized using alkaline phosphatase coupled anti-mouse IgG.

The models of RPE65 tertiary structure show protein core regions containing significant beta pleated sheet content, with the major difference being that the Rosetta-based model is much less compact than the Swiss-based model based the solved structure of apocarotenoid-cleaving oxygenase. This finding is not unexpected since the ab initio methods used for the Rosetta-based model are capable of producing roughly correct models with complex topologies, however, accuracy diminishes for large structures unassociated with a protein family [44,45]. In each independently derived model, known patient missense mutations appear distributed throughout the tertiary structure, with no regional clustering evident. In addition, the KVNPETLETI sequence recognized by mAb 8B11, and the FHHINTYEDNGFLIV sequence used to elicit mAb 1F9, both localize to surface exposed loops that are relatively unstructured. No predicted sites of posttranslational modifications or patient mutations are present within the mAb 8B11 antigenic determinant. However, the mAb 1F9 peptide contains both sites of patient mutations (N321K, 962-963 ins A) and potential interaction with metal ions (His313).

Immunohistochemical analysis of species and tissue specificity: To establish the specificity of RPE65 expression in

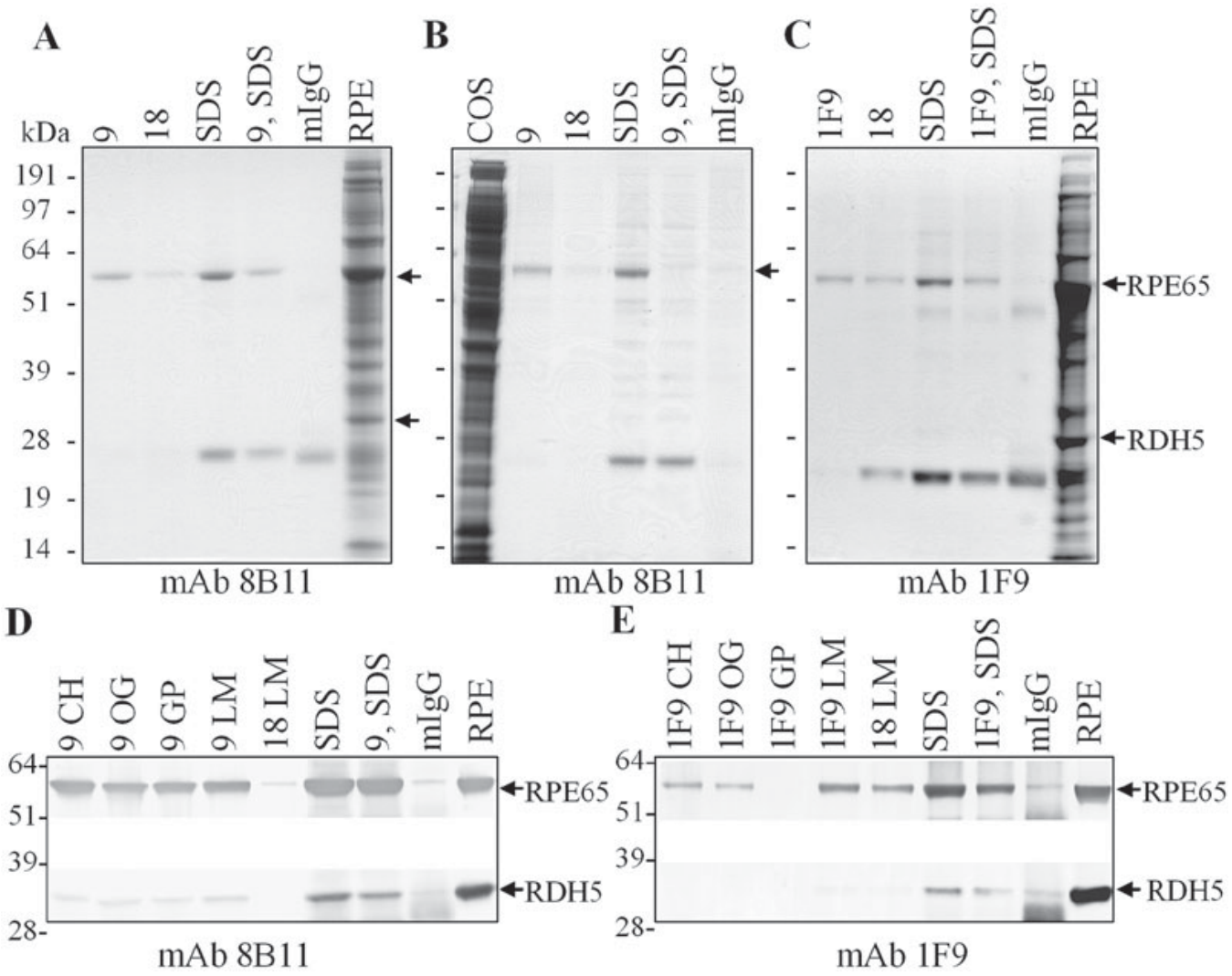

Figure 6. RPE65 immunoabsorption and peptide elution. **A**,**B**,**C**: Bovine RPE membranes in CHAPS (**A**), COS-7 cells transfected with an RPE65 cDNA expression construct in CHAPS (**B**), or bovine RPE membranes in laurylmaltoside (**C**) were incubated with mAb 8B11-Sepharose (**A**,**B**), or with mAb 1F9-Sepharose (**C**). Coomassie blue stained gels of proteins eluted with peptide 9 corresponding to the mAb 8B11 epitope (**A**,**B**), with the FHHINTYEDNGFLIV peptide used to generate mAb 1F9 (**C**), with peptide 18 corresponding to an RPE65 sequence that did not compete in ELISA's, or with SDS-sample buffer. **D**,**E**: Western analysis of bovine RPE membranes in various detergents immunoabsorbed on mAb 8B11-Sepharose (**D**), or on mAb 1F9-Sepharose (**E**), and eluted with peptides or SDS-sample buffer, as shown. Proteins were transferred to nitrocellulose and probed with mAb 8B11 (**D**), mAb 1F9 (**E**), or an antibody against RDH5 (**D**,**E**), and reactivity visualized using alkaline phosphatase coupled anti-mouse IgG. Arrows indicate the positions of RPE65 and RDH5. CH represents CHAPS; OC represents octylglucoside; GP represents Genapol; LM represents laurylmaltoside; mIgG represents nonspecific mIgG-Sepharose matrix; 9 represents KVNPETLETI; 1F9 represents FHHINTYEDNGFLIV; 9, SDS represents peptide 9 eluted matrix subsequently eluted by SDS; 1F9, SDS represents peptide 1F9 eluted matrix subsequently eluted with SDS.

A

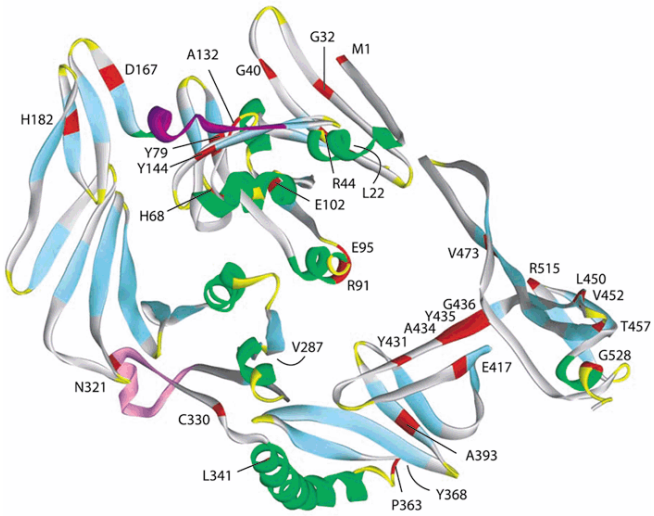

B

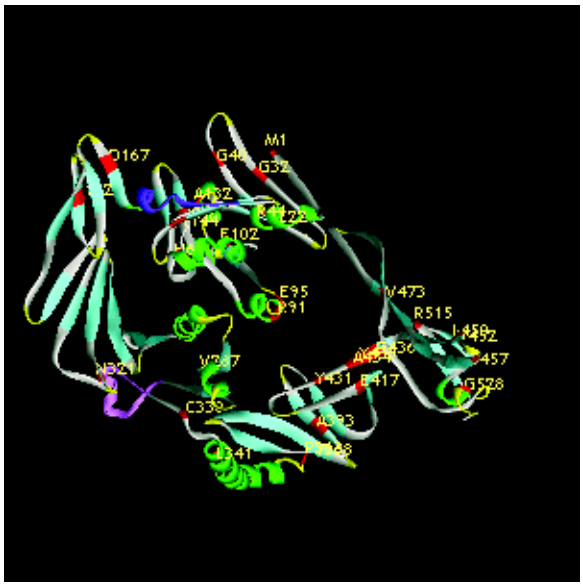

Figure 7. Ab initio model of RPE65 tertiary structure. **A**: A three-dimensional structure for the RPE65 protein was predicted using the method of Bystroff and Shao [39]. The ribbon representing the peptide backbone is color coded according to structural components: α-helices are green; β-pleated sheets are blue; and random coil is gray. The linear sequence corresponding to the epitope recognized by mAb 8B11 is shown in purple and for mAb 1F9 is shown in pink. Sites of amino acid substitutions resulting from patient missense mutations associated with inherited retinal degeneration in patients are shown in red. **B**: The structure is animated in the online version of this article at the following URL: http://www.molvis.org/molvis/v11/a133/hemati-fig7.html.

A

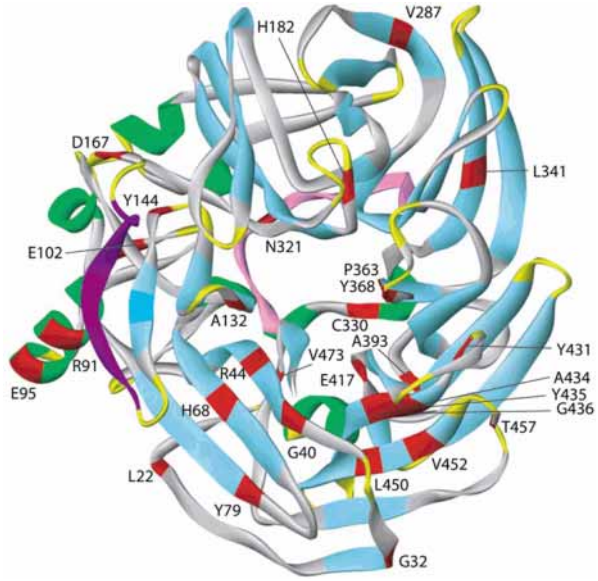

B

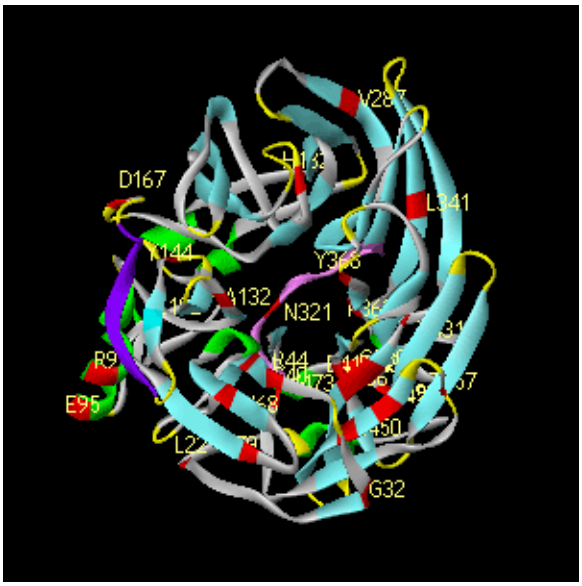

Figure 8. Correlative model of RPE65 tertiary structure. **A**: A three-dimensional structure for the RPE65 protein was predicted by comparison to the apocarotenoid-cleaving oxygenase from Synechocystis and modeled by the SWISS-MODEL server [43]. The ribbon representing the peptide backbone is color coded according to structural components: α-helices are green; β-pleated sheets are blue; and random coil is gray. The linear sequence corresponding to the epitope recognized by mAb 8B11 is shown in purple and for mAb 1F9 is shown in pink. Sites of amino acid substitutions resulting from patient missense mutations associated with inherited retinal degeneration in patients are shown in red. **B**: The structure is animated in the online version of this article at the following URL: http://www.molvis.org/molvis/v11/a133/hemati-fig8.html.

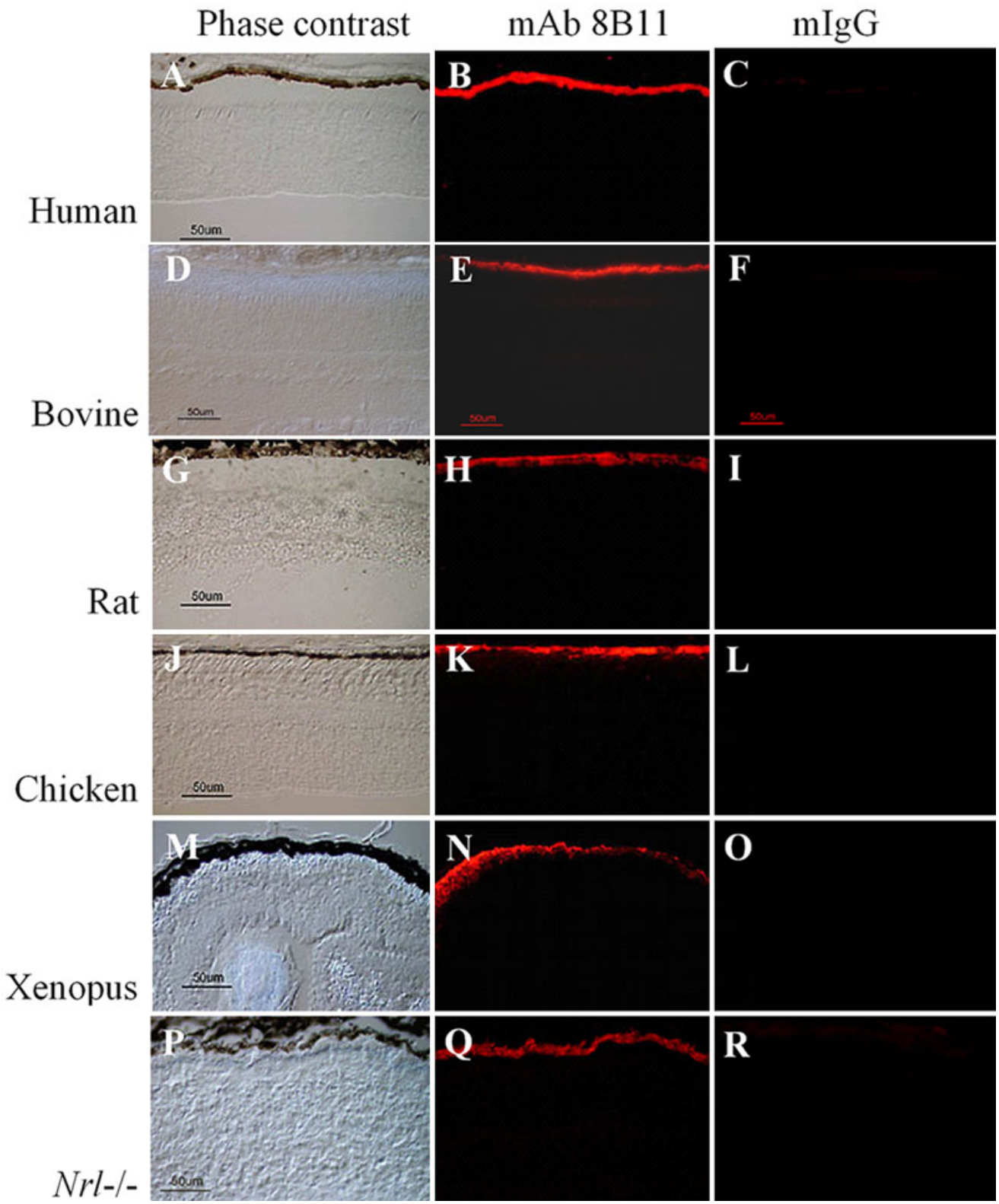

Figure 9. Immunohistochemical analysis of mAb 8B11 reactivity in rod- and cone-dominant retinas. Retina/choroid/RPE cryosections of paraformaldehyde-fixed eyes from bovine, human, rat (rod-dominant), and from *Xenopus laevis*, chicken, *Nrl* knockout mouse (cone-dominant) were incubated with mAb 8B11 or mouse non-immune IgG, and immunoreactivity was visualized with Alexa Fluor 555-conjugated anti-mouse IgG using fluorescence imaging. Retina/choroid/RPE cryosections from paraformaldehyde eyes were incubated with mAb 8B11 or mouse non-immune IgG, and reactivity was visualized with Alexa Fluor 555-conjugated anti-mouse IgG using fluorescence imaging. Phase contrast (**A**,**D**,**G**,**J**,**M**,**P**), mAb 8B11 reactivity (**B**,**E**,**H**,**K**,**N**,**Q**), non-immune mouse IgG reactivity (**C**,**F**,**I**,**L**,**O**,**R**). Bovine sections are from an amelanotic region of the RPE. The scale bars represent 50 μm.

eyes with rod- and cone-dominant retinas, mAb 8B11 and mAb 1F9 reactivity was assessed using immunohistochemical analysis of retina/RPE/choroid or whole globe cryosections from various species. With mAb 8B11, intense reactivity restricted to the RPE layer was seen in human, bovine, and rat; all species having rod dominant retinas (Figure 9). mAb 8B11 reactivity was also seen only in the RPE in chicken and *Xenopus laevis* whose retinas contain a high ratio of cone to rod cells, as well as in *Nrl* knockout mice whose retinas contain exclusively cone-like photoreceptor cells [46-49]. With mAb 1F9, immunoreactivity confined to the RPE layer was seen in human, bovine, and the *Nrl* knockout mouse (Figure 10). However, mAb 1F9 reactivity was completely absent in chicken and *Xenopus*, apparently due to lack of crossreactivity with RPE65 protein from these species as a result of sequence differences.

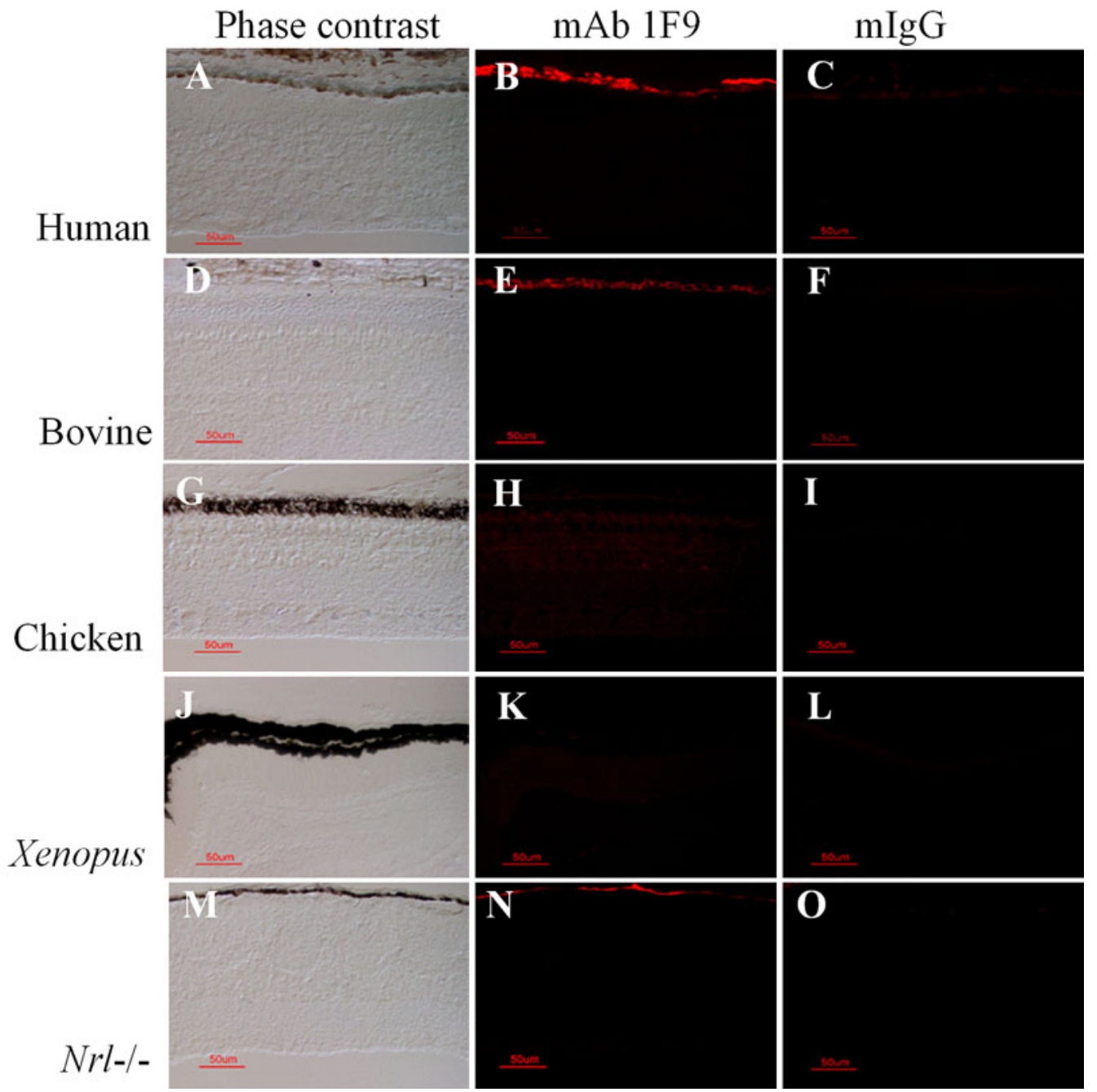

Figure 10. Immunohistochemical analysis of mAb 1F9 reactivity in rod- and cone-dominant retinas. Retina/choroid/RPE cryosections of paraformaldehyde-fixed eyes from bovine, human (rod-dominant), and from *Xenopus laevis*, chicken, *Nrl* knockout mouse (cone-dominant) were incubated with mAb 1F9 or mouse non-immune IgG using M.O.M. Peroxidase reagents, and visualized using TSA-Alexa fluor 568 reagents using fluorescence imaging (1/50 s human, all others 1/30 s). Phase contrast (**A**,**D**,**G**,**J**,**M**), mAb 1F9 reactivity (**B**,**E**,**H**,**K**,**N**), non-immune mouse IgG reactivity (**C**,**F**,**I**,**L**,**O**). Bovine sections are from an amelanotic region of the RPE. The scale bars represent 50 μm.

The reactivity of mAb 8B11 and mAb 1F9 was also evaluated in retina flatmounts and compared to the pattern of cone labeling using PNA-lectin, as well as to the reactivity of antibodies against S-opsin and M/L-opsin present in the cone photoreceptor outer segments (Figure 11). Retinas were from wild type mice (B6/129), from *Rpe65* knockout mice in which no protein is detected [2], and from *Nrl* knockout mice. Conditions for tissue preparation and labeling were similar to those used by Znoiko et al. [19]. In all three mouse genotypes, no RPE65 reactivity could be seen in cones or any other cells of the retina using either antibody, establishing that the absence of signal in retina/RPE/choroid sections was not due to masking by the intense signal from the RPE.

DISCUSSION

We have developed and characterized two monoclonal antibodies specific for RPE65 that recognize independent antigenic determinants present on the surface of the native protein. In the case of mAb 8B11 elicited using RPE membranes as immunogen, the corresponding antigenic determinant, KVNPETLETI, is conserved among bovine, newt, and frog RPE65 orthologs, and differs only at the second position (Ile is Val) in human, monkey, rat, mouse, dog, chicken, and salamander. As a result, this high affinity antibody is an effective tool for studies of RPE65 from a number of species, exhibiting cross-reactivity with all vertebrates tested so far. It is interesting to note that, in previous studies by others to develop RPE65 antibodies by immunization with synthetic peptides, the most effective antibody obtained was elicited by 150-NFITKVNPETLETIK-164 containing the epitope recognized by mAb 8B11 [50]. The convergence of two different ap-

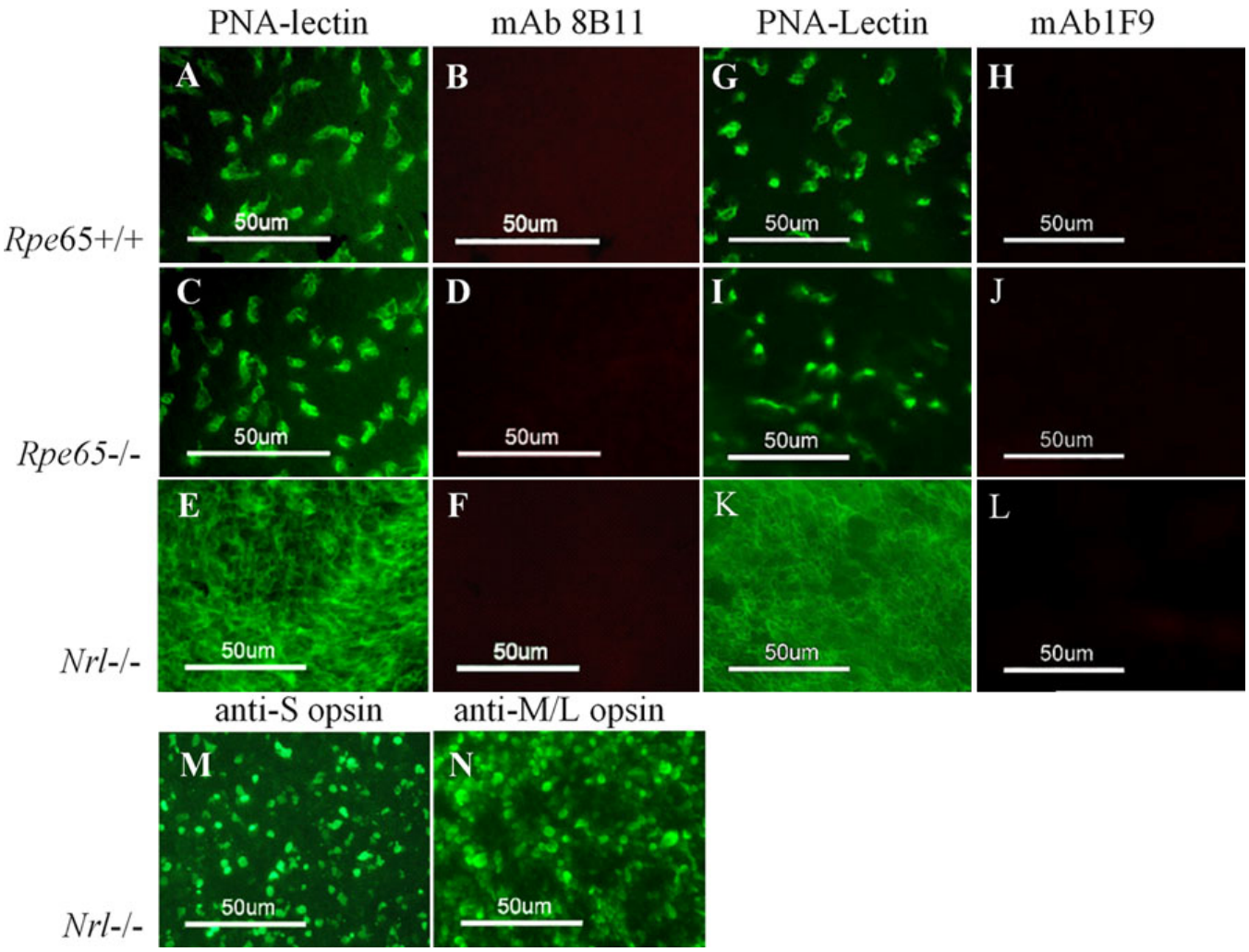

Figure 11. Immunohistochemical analysis of retina flatmounts. Retinas from wild type (**A**,**B**,**G**,**H**), Rpe65 knockout (**C**,**D**,**I**,**J**), and *Nrl* knockout mouse (**E**,**F**,**K**-**N**) were fixed on coverslips and incubated with PNA-lectin (FITC-conjugated), mAb 8B11, mAb 1F9, or antibodies against S-opsin and M/L-opsin. Alexa Fluor 555-conjugated anti-mouse IgG was used as secondary antibody. PNA labeling (**A**,**C**,**E**,**G**,**I**,**K**), mAb 8B11 labeling (**B**,**D**,**F**), mAb 1F9 labeling (**H**,**J**,**L**), S-opsin labeling (**M**), M/L-opsin labeling, (**N**). Fluorescence imaging: PNA-lectin, opsin antibodies 1/60 s; mAb 8B11 1/12 s; mAb 1F9, 1/20 s. The scale bars represent 50 μm.

proaches to RPE65 antibody production on the same amino acid sequence suggests that this region of the protein is highly antigenic. We have now shown that a second human RPE65 sequence, FHHINTYEDNGFLIV, is also relatively antigenic. The corresponding mAb 1F9 exhibits specificity similar to that of mAb 8B11, but has apparently lower affinity and a narrower range of cross-species reactivity, most likely due to coding sequence differences between species.

Consistent with our use of native RPE membranes as antigen, as well as predictions of hydrophilicity and antigenicity, the antigenic determinants recognized by mAb 8B11 and mAb 1F9 were found to be amino acid sequences likely to be present on the RPE65 protein surface. The ability of each antibody to recognize native RPE65 solubilized in non-ionic detergents made it possible to develop immunoaffinity purification protocols effective in purifying RPE65 from bovine RPE membranes, and from transfected COS-7 cells expressing the recombinant protein. Establishing the surface accessibility of the KVNPETLETI and FHHINTYEDNGFLIV epitopes represents a first step toward validating predicted models of RPE65 tertiary structure derived using ab initio and comparative methods, thus confirming the potential usefulness of such models for guiding future experimental design.

Preparations of RPE65 purified from bovine RPE membranes using mAb 8B11 or mAb 1F9 immunoaffinity chromatography were found to contain co-eluted RDH5 that could be seen by western analysis. Only small amounts of RDH5 were present, even when washes were performed in the cold using minimum times and volumes and various detergents. RDH5 is an abundant protein in the RPE that appears to undergo significant nonspecific interaction with the affinity matrix solid support. However, two other visual processing proteins, RGR and LRAT, that are relatively abundant and likely to functionally interact with RPE65, were not detected in immunoaffinity purified material. It therefore seems likely that the co-purification of RDH5 with RPE65 reflects a high affinity association of these proteins in vivo, rather than a nonspecific effect. This finding is in agreement with previous studies that reported that RDH5 co-purifies with RPE65 when nonspecific methods of elution (e.g. high pH) are used [51]. Further studies will be needed to determine whether RPE65 and RDH5 exist in a stable retinoid processing complex in vivo.

Our analysis of mAb 8B11 immunoreactivity in eye cross-sections and retina flatmounts detected RPE65 expression only in the RPE in a number of species that have rod- or cone-dominant retinas, including *Xenopus laevis* (approx. 40% cones [52]), chicken (approx. 60% cones [53]), and the *Nrl* knockout mouse in which the cone-like phenotype of the photoreceptor cells has been established on the basis of a number of morphological, molecular, and electrophysiological criteria that distinguish the photoreceptors from rods [46-49]. Corroborating data was obtained using mAb 1F9 to assess immunoreactivity in mouse, human, and *Nrl* knockout mouse. Our finding of RPE65 expression only in the RPE and not in retina is in agreement with an earlier study that specifically addressed this issue in the mouse [54]. In contrast, studies by Ma and coworkers reported RPE65 expression in cones; first finding RPE65 mRNA in salamander cones using reverse transcriptase-coupled polymerase chain reaction [55], and then finding RPE65 immunoreactivity in mouse, bovine, rabbit, and *Xenopus laevis* retina flatmounts using polyclonal antibody elicited against 150-NFITKVNPETLETIK-164 [19]. Curiously, in the second study, a higher density of labeled cells was seen in rod-dominant mouse, bovine, and rabbit retinas than in *Xenopus laevis* retinas that are comprised of 30% cones, an apparent incongruity not discussed by the authors. Signficantly, the reactivity of preimmune serum on the retina flatmounts was not shown. Our studies do not exclude the possibility that very low level expression of RPE65 exists outside the RPE. In fact, in a recent study, low level RPE65 expression in the ciliary body was detected using RT-PCR and western analysis, but not by immunohistochemistry [56].

We conclude that the primary site of RPE65 function is in the RPE-based visual cycle, finding no physical evidence to suggest a direct role in an alternate visual cycle present in cone cells. The identification of two distinct RPE65 surface epitopes represents a first step toward developing a structural understanding of this important disease gene product. Future goals will be to define the nature of the RPE65 domains involved in interactions with other proteins that participate in vitamin A processing in the RPE, as well as in catalysis and substrate binding, and to understand the impact of specific patient mutations on these structures. mAb 8B11 and mAb 1F9 should prove to be useful tools in many such studies.

ACKNOWLEDGEMENTS

The authors would like to thank Anand Swaroop and Alan J. Mears for *Nrl* knockout mice, T. Michael Redmond for *Rpe65* knockout mice, Krzyztof Palczewski for antibody against 11-*cis* retinol dehydrogenase (RDH5), Henry Fong for antibody against retinal G protein-coupled receptor (RGR), Dean Bok for antibody against lecithin retinol acyl transferase (tLRAT), and Jill Baney and Elizabeth Smith (MDRTC Hybridoma Core Facility) and Mitchell Gillett (Vision Morphology Core) for expert technical assistance. Grant support: National Institutes of Health Grant R01-EY12298 (DAT), P30-EY07003 (Vision Research Core Grant), P60DK-20572 (Michigan Diabetes Research and Training Center Grant), M01-RR00042 (General Clinical Research Center), Foundation Fighting Blindness (DAT), Research to Prevent Blindness (DAT). Presented in part at the annual meetings of the Association for Research in Vision and Ophthalmology, Ft. Lauderdale, FL, May 2003.

REFERENCES

1. Hamel CP, Tsilou E, Pfeffer BA, Hooks JJ, Detrick B, Redmond TM. Molecular cloning and expression of RPE65, a novel retinal pigment epithelium-specific microsomal protein that is post-transcriptionally regulated in vitro. J Biol Chem 1993; 268:15751-7.
2. Redmond TM, Yu S, Lee E, Bok D, Hamasaki D, Chen N, Goletz P, Ma JX, Crouch RK, Pfeifer K. Rpe65 is necessary for production of 11-cis-vitamin A in the retinal visual cycle. Nat Genet 1998; 20:344-51.
3. Manes G, Leducq R, Kucharczak J, Pages A, Schmitt-Bernard CF, Hamel CP. Rat messenger RNA for the retinal pigment epithe-

lium-specific protein RPE65 gradually accumulates in two weeks from late embryonic days. FEBS Lett 1998; 423:133-7.
4. Thompson DA, Gal A. Vitamin A metabolism in the retinal pigment epithelium: genes, mutations, and diseases. Prog Retin Eye Res 2003; 22:683-703.
5. Van Hooser JP, Aleman TS, He YG, Cideciyan AV, Kuksa V, Pittler SJ, Stone EM, Jacobson SG, Palczewski K. Rapid restoration of visual pigment and function with oral retinoid in a mouse model of childhood blindness. Proc Natl Acad Sci U S A 2000; 97:8623-8.
6. Acland GM, Aguirre GD, Ray J, Zhang Q, Aleman TS, Cideciyan AV, Pearce-Kelling SE, Anand V, Zeng Y, Maguire AM, Jacobson SG, Hauswirth WW, Bennett J. Gene therapy restores vision in a canine model of childhood blindness. Nat Genet 2001; 28:92-5.
7. Narfstrom K, Katz ML, Bragadottir R, Seeliger M, Boulanger A, Redmond TM, Caro L, Lai CM, Rakoczy PE. Functional and structural recovery of the retina after gene therapy in the RPE65 null mutation dog. Invest Ophthalmol Vis Sci 2003; 44:1663-72.
8. Jin M, Li S, Moghrabi WN, Sun H, Travis GH. Rpe65 is the retinoid isomerase in bovine retinal pigment epithelium. Cell 2005; 122:449-59.
9. Moiseyev G, Chen Y, Takahashi Y, Wu BX, Ma JX. RPE65 is the isomerohydrolase in the retinoid visual cycle. Proc Natl Acad Sci U S A 2005; 102:12413-8.
10. Redmond TM, Poliakov E, Yu S, Tsai JY, Lu Z, Gentleman S. Mutation of key residues of RPE65 abolishes its enzymatic role as isomerohydrolase in the visual cycle. Proc Natl Acad Sci U S A 2005; 102:13658-63.
11. Deigner PS, Law WC, Canada FJ, Rando RR. Membranes as the energy source in the endergonic transformation of vitamin A to 11-cis-retinol. Science 1989; 244:968-71.
12. Gollapalli DR, Maiti P, Rando RR. RPE65 operates in the vertebrate visual cycle by stereospecifically binding all-trans-retinyl esters. Biochemistry 2003; 42:11824-30. Erratum in: Biochemistry 2004; 43:7226.
13. Mata NL, Moghrabi WN, Lee JS, Bui TV, Radu RA, Horwitz J, Travis GH. Rpe65 is a retinyl ester binding protein that presents insoluble substrate to the isomerase in retinal pigment epithelial cells. J Biol Chem 2004; 279:635-43.
14. Xue L, Gollapalli DR, Maiti P, Jahng WJ, Rando RR. A palmitoylation switch mechanism in the regulation of the visual cycle. Cell 2004; 117:761-71.
15. Woodruff ML, Wang Z, Chung HY, Redmond TM, Fain GL, Lem J. Spontaneous activity of opsin apoprotein is a cause of Leber congenital amaurosis. Nat Genet 2003; 35:158-64.
16. Rohrer B, Ablonczy Z, Znoiko S, Redmond M, Ma JX, Crouch R. Does constitutive phosphorylation protect against photoreceptor degeneration in Rpe65-/- mice? Adv Exp Med Biol 2003; 533:221-7.
17. Mata NL, Radu RA, Clemmons RC, Travis GH. Isomerization and oxidation of vitamin a in cone-dominant retinas: a novel pathway for visual-pigment regeneration in daylight. Neuron 2002; 36:69-80.
18. Das SR, Bhardwaj N, Kjeldbye H, Gouras P. Muller cells of chicken retina synthesize 11-cis-retinol. Biochem J 1992; 285:907-13.
19. Znoiko SL, Crouch RK, Moiseyev G, Ma JX. Identification of the RPE65 protein in mammalian cone photoreceptors. Invest Ophthalmol Vis Sci 2002; 43:1604-9.
20. Nicoletti A, Wong DJ, Kawase K, Gibson LH, Yang-Feng TL, Richards JE, Thompson DA. Molecular characterization of the human gene encoding an abundant 61 kDa protein specific to the retinal pigment epithelium. Hum Mol Genet 1995; 4:641-9.
21. Porto FB, Perrault I, Hicks D, Rozet JM, Hanoteau N, Hanein S, Kaplan J, Sahel JA. Prenatal human ocular degeneration occurs in Leber's congenital amaurosis (LCA2). J Gene Med 2002; 4:390-6.
22. Valeria Canto Soler M, Gallo JE, Dodds RA, Suburo AM. A mouse model of proliferative vitreoretinopathy induced by dispase. Exp Eye Res 2002; 75:491-504.
23. Tan E, Ding XQ, Saadi A, Agarwal N, Naash MI, Al-Ubaidi MR. Expression of cone-photoreceptor-specific antigens in a cell line derived from retinal tumors in transgenic mice. Invest Ophthalmol Vis Sci 2004; 45:764-8.
24. West KA, Yan L, Miyagi M, Crabb JS, Marmorstein AD, Marmorstein L, Crabb JW. Proteome survey of proliferating and differentiating rat RPE-J cells. Exp Eye Res 2001; 73:479-91.
25. Mircheff AK, Miller SS, Farber DB, Bradley ME, O'Day WT, Bok D. Isolation and provisional identification of plasma membrane populations from cultured human retinal pigment epithelium. Invest Ophthalmol Vis Sci 1990; 31:863-78.
26. Heller J, Jones P. Purification of bovine retinal pigment epithelial cells by dissociation in calcium free buffers and centrifugation in Ficoll density gradients followed by "recovery" in tissue culture. Exp Eye Res 1980; 30:481-7.
27. Claflin JL, Hudak S, Maddalena A. Anti-phosphocholine hybridoma antibodies. I. Direct evidence for three distinct families of antibodies in the murine response. J Exp Med 1981; 153:352-64.
28. Gefter ML, Margulies DH, Scharff MD. A simple method for polyethylene glycol-promoted hybridization of mouse myeloma cells. Somatic Cell Genet 1977; 3:231-6.
29. Kearney JF, Radbruch A, Liesegang B, Rajewsky K. A new mouse myeloma cell line that has lost immunoglobulin expression but permits the construction of antibody-secreting hybrid cell lines. J Immunol 1979; 123:1548-50.
30. Birk HW, Koepsell H. Reaction of monoclonal antibodies with plasma membrane proteins after binding on nitrocellulose: renaturation of antigenic sites and reduction of nonspecific antibody binding. Anal Biochem 1987; 164:12-22.
31. Harlow E, Lane D. Antibodies: a laboratory manual. Cold Spring Harbor (NY): Cold Spring Harbor Laboratory; 1988.
32. Chirgwin JM, Przybyla AE, MacDonald RJ, Rutter WJ. Isolation of biologically active ribonucleic acid from sources enriched in ribonuclease. Biochemistry 1979; 18:5294-9.
33. Hodges RS, Heaton RJ, Parker JM, Molday L, Molday RS. Antigen-antibody interaction. Synthetic peptides define linear antigenic determinants recognized by monoclonal antibodies directed to the cytoplasmic carboxyl terminus of rhodopsin. J Biol Chem 1988; 263:11768-75.
34. Saari JC, Bredberg DL. Acyl-CoA:retinol acyltransferase and lecithin:retinol acyltransferase activities of bovine retinal pigment epithelial microsomes. Methods Enzymol 1990; 190:156-63.
35. Haeseleer F, Jang GF, Imanishi Y, Driessen CA, Matsumura M, Nelson PS, Palczewski K. Dual-substrate specificity short chain retinol dehydrogenases from the vertebrate retina. J Biol Chem 2002; 277:45537-46.
36. Pandey S, Blanks JC, Spee C, Jiang M, Fong HK. Cytoplasmic retinal localization of an evolutionary homolog of the visual pigments. Exp Eye Res 1994; 58:605-13.
37. Bok D, Ruiz A, Yaron O, Jahng WJ, Ray A, Xue L, Rando RR. Purification and characterization of a transmembrane domain-

deleted form of lecithin retinol acyltransferase. Biochemistry 2003; 42:6090-8.
38. Oprian DD, Molday RS, Kaufman RJ, Khorana HG. Expression of a synthetic bovine rhodopsin gene in monkey kidney cells. Proc Natl Acad Sci U S A 1987; 84:8874-8.
39. Bystroff C, Shao Y. Fully automated ab initio protein structure prediction using I-SITES, HMMSTR and ROSETTA. Bioinformatics 2002; 18 Suppl 1:S54-61.
40. Bystroff C, Thorsson V, Baker D. HMMSTR: a hidden Markov model for local sequence-structure correlations in proteins. J Mol Biol 2000; 301:173-90.
41. Simons KT, Bonneau R, Ruczinski I, Baker D. Ab initio protein structure prediction of CASP III targets using ROSETTA. Proteins 1999; Suppl 3:171-6.
42. Kloer DP, Ruch S, Al-Babili S, Beyer P, Schulz GE. The structure of a retinal-forming carotenoid oxygenase. Science 2005; 308:267-9.
43. Schwede T, Kopp J, Guex N, Peitsch MC. SWISS-MODEL: An automated protein homology-modeling server. Nucleic Acids Res 2003; 31:3381-5.
44. Bonneau R, Strauss CE, Rohl CA, Chivian D, Bradley P, Malmstrom L, Robertson T, Baker D. De novo prediction of three-dimensional structures for major protein families. J Mol Biol 2002; 322:65-78.
45. Bradley P, Chivian D, Meiler J, Misura KM, Rohl CA, Schief WR, Wedemeyer WJ, Schueler-Furman O, Murphy P, Schonbrun J, Strauss CE, Baker D. Rosetta predictions in CASP5: successes, failures, and prospects for complete automation. Proteins 2003; 53 Suppl 6:457-68.
46. Mears AJ, Kondo M, Swain PK, Takada Y, Bush RA, Saunders TL, Sieving PA, Swaroop A. Nrl is required for rod photoreceptor development. Nat Genet 2001; 29:447-52.
47. Strettoi E, Mears AJ, Swaroop A. Recruitment of the rod pathway by cones in the absence of rods. J Neurosci 2004; 24:7576-82.
48. Daniele LL, Lillo C, Lyubarsky AL, Nikonov SS, Philp N, Mears AJ, Swaroop A, Williams DS, Pugh EN Jr. Cone-like morphological, molecular, and electrophysiological features of the photoreceptors of the Nrl knockout mouse. Invest Ophthalmol Vis Sci 2005; 46:2156-67.
49. Nikonov SS, Daniele LL, Zhu X, Craft CM, Swaroop A, Pugh EN Jr. Photoreceptors of Nrl -/- mice coexpress functional S- and M-cone opsins having distinct inactivation mechanisms. J Gen Physiol 2005; 125:287-304.
50. Redmond TM, Hamel CP. Genetic analysis of RPE65: from human disease to mouse model. Methods Enzymol 2000; 316:705-24.
51. Simon A, Hellman U, Wernstedt C, Eriksson U. The retinal pigment epithelial-specific 11-cis retinol dehydrogenase belongs to the family of short chain alcohol dehydrogenases. J Biol Chem 1995; 270:1107-12.
52. Wilhelm M, Gabriel R. Functional anatomy of the photoreceptor and second-order cell mosaics in the retina of Xenopus laevis. Cell Tissue Res 1999; 297:35-46.
53. Meyer DB, May HC Jr. The topographical distribution of rods and cones in the adult chicken retina. Exp Eye Res 1973; 17:347-55.
54. Seeliger MW, Grimm C, Stahlberg F, Friedburg C, Jaissle G, Zrenner E, Guo H, Reme CE, Humphries P, Hofmann F, Biel M, Fariss RN, Redmond TM, Wenzel A. New views on RPE65 deficiency: the rod system is the source of vision in a mouse model of Leber congenital amaurosis. Nat Genet 2001; 29:70-4.
55. Ma J, Xu L, Othersen DK, Redmond TM, Crouch RK. Cloning and localization of RPE65 mRNA in salamander cone photoreceptor cells1. Biochim Biophys Acta 1998; 1443:255-61.
56. Salvador-Silva M, Ghosh S, Bertazolli-Filho R, Boatright JH, Nickerson JM, Garwin GG, Saari JC, Coca-Prados M. Retinoid processing proteins in the ocular ciliary epithelium. Mol Vis 2005; 11:356-65.

The print version of this article was created on 21 Dec 2005. This reflects all typographical corrections and errata to the article through that date. Details of any changes may be found in the online version of the article.